29456 DUP.

IGM88AP-103-778-G
CNRC 29456

TENSILE PROPERTIES OF INJECTION MOLDED LONG FIBER THERMOPLASTIC COMPOSITES

J. Denault, T. Vu-Khanh, B. Foster

INDUSTRIAL MATERIALS RESEARCH INSTITUTE

National Research Council Canada

75 De Mortagne

Boucherville, Quebec, Canada J4B 6Y4

TENSILE PROPERTIES OF INJECTION MOLDED LONG FIBER THERMOPLASTIC COMPOSITES

J. Denault, T. Vu-Khanh, B. Foster

INDUSTRIAL MATERIALS RESEARCH INSTITUTE
National Research Council Canada
75 De Mortagne
Boucherville, Quebec, Canada J4B 6Y4

ABSTRACT

This paper deals with the mechanical performances of a new class of injection molded long fiber composites based on PP and PBT matrices. Effects of material parameters such as fiber concentration, breakage, orientation and matrix composition are analysed. The critical fiber length, l_c, of the PP long fiber composite, evaluated from the pull-out length of the tensile fracture surface was found to be much higher than those which are previously reported. Tensile strength calculated from the measured l_c and fiber length distribution in the moulded samples was found in agreement with the measured values. From this work it is concluded that higher mechanical performances of the long fiber reinforced thermoplastics will be attained by the injection molding process to further reduce fiber breakage.

INTRODUCTION

Since the advent of a new impregnation technology, discontinuous fiber thermoplastic composites which offer high specific strength and stiffness can be easily processed by injection molding into complex shaped parts (1). This new kind of injection grade of fiber reinforced thermoplastic is obtained by impregnating continuous fiber strands with matrix resin followed by chopping. This impregnation technique led to the production of fully compounded long fiber thermoplastic composites, i.e. all filaments are well separated and coated with matrix (see Figure 1). Furthermore, the reinforcing fibers extend to the entire length of chopped pellet, usually 12 mm. Injection molding of these long fiber pellets leads to composite in which fiber length is much higher than that in conventional injection grades of reinforced thermoplastics, obtained by the extrusion process as a melt-bending method (2). The retention of fiber length in the finished part leads to materials with higher performance.

Although mechanical behavior of short fiber reinforced thermoplastics has been greatly investigated in the past (3-11) and also well reviewed (12-14), the advent of "long fiber" thermoplastic composites requires equivalent evaluation. The purpose of the present study is to characterize the tensile behavior of the injection molded long fiber composite based on polypropylene and polybutylene terephtalate. Effect of matrix composition, fiber length distribution, fiber orientation and fiber volume content on the stiffness and the tensile strength were

investigated. The tensile properties were interpreted in term of the interfacial shear strength determined by the measurement of the fiber pull-out length on the fractured specimen. Strength of the composites is predicted using the modified rule of mixtures. Effect of pellet dilution on fiber degradation during processing was also investigated.

EXPERIMENTAL

Long fiber composites investigated in this study are based on two different thermoplastic matrices; polybutylene terephtalate and polypropylene, supplied by Bay Mills Canada and Celanese repectively. In the objective of studying the effect of fiber concentration in these materials, samples of varying composition were obtained by dry blending long fiber pellets with pellets of pure resin.

Long fiber pellets of PBT and PP of respectively 12 mm and 13 mm were processed using a standard injection molding press. However, in view of preventing high fiber breakage during the injection moulding, nozzle of 7.9 mm diameter, runner system of 6.4 mm in diameter and large rectangular gates of 6.4 mm X 3.2 mm were used. Tensile test pieces (ASTM D-638, Type 1) and rectangular plates of 6 mm X 27 mm X 124 mm were molded.

A scanning electron microscope (Type Jeol 35CF) was used for the microstructural analysis. Tensile tests were performed on a standard testing machine (Instron, Model 1125) with cross-head speed of 1 mm/min and the deformations were measured by a strain gage extensiometer

Instron Model No. A325-242630-004, having a gage length of 25.4 mm.

Fiber degradation during the injection molding process was characterized by the measure of fiber length distribution in the moulded samples. Due to the wide range of fiber lengths present in the sample (0.3 to 13 mm), two different techniques were used to construct the complete distribution. Glass fibers were isolated from the sample by burning off the resin in an oven and thereafter separated in two portions ($\lesssim$ 1 mm and $\gtrsim$1 mm) by sieving. The amount of fiber in each fraction was weighed and analysed to determine the number and length. The fraction of short fiber ($\lesssim$ 1 mm) was analysed with an automatic particle size analyser PA-720 HIAC Pacific Scientific adapted for fibers analysis (15). The fraction of long fiber ($>$ 1 mm) was analysed with a semi-automatic image analyser developed in our laboratory (16). The two fiber length distributions were combined in consideration of their relative weight. The complete fiber length distribution was obtained after analysing approximately 5000 fibers $\lesssim$ 1 mm and 2000 fiber $\gtrsim$ 1 mm.

RESULTS AND DISCUSSION

In view to obtain long fiber composites with optimum mechanical performances, great attention was made to minimize fiber breakage during injection molding. Recently, Ciannelli *etal* (17) have published a detailed study to quantify the effects of processing variables and equipment on moulded properties and fiber length distribution. Following the results of this study, all of the long fiber composites were moulded at low shear and at high temperature (540°C PBT and 400°C for PP) using a

descending barrel-temperature profiles. In fact, the objective is to melt the pellets immediately by using external heat rather than shear heat, which would lead to increase fiber damage.

Fiber length

Fiber length distribution in PBT and PP composites of different compositions are shown in Figures 2 and 3, respectively. From these figures, it can be concluded that fiber degradation during the injection molding process is greatly dependent on the long fiber concentration. Increasing long fiber content in PBT and PP matrix results in a reduction of the number average fiber length in the sample (see Table I). Higher melt viscosity as well as higher fiber contact during injection molding of the concentrated system could probably be responsible for a more severe damage. However, in spite of the obvious reduction of fiber length in the highly filled system, fibers of length up to 10 mm are present in these samples. It can also be observed that all distribution curves show a large degree of skewness towards higher length regions, indicating the presence of significative proportion of long fiber fragments.

Polybutylene terephtalate composites of 4.9%, 11.1% and 19.0% fiber volume content were prepared by dilution of pellets of 54% by volume and, PP composites of 2.0% and 7.9% were obtained by dilution of pellets at 15% by volume. The efficiency of the dilution procedure can be observed in Figure 4 showing the tensile fracture surfaces of long fiber reinforced PBT of composition of 4.9% and 11.1%. Good fiber dispersion in the

injection moulded samples insure the efficiency of the dilution technique.

Qualitative characterization of fiber orientation in the long fiber composite of various fiber content was made by microscopic observation of polished sample, in a scanning electron microscope. Micrographs of polished transverse section of the moulded samples (ASTM D638, Type 1) of PP and PBT of different compositions are shown in Figure 5. From this figure, it can be observed that an increase in fiber concentration produces a reduction in fiber orientation in the moulding. It can also be observed that the orientation pattern in the PP composites is different from the PBT composites. The region of misalignment in PP seems to be more extended than that in PBT. This possibly results from longer fiber in the PP composites. These microscopic observations also permit to detect the presence of holes in the PP composite of 36.4 vol.% while PBT composites from all composition were found to be homogeneous. Holes will probably lead to materials of lower performance than expected.

Fracture Mechanism

Figure 6 shows the variation of the percentage of elongation at break of long fiber reinforced PBT and PP as a function of fiber concentration. All of the long fiber composites were found to break in a brittle manner. In addition, the fracture occurs at strains lower than fiber failure strains of 3%. This brittle behavior has also been observed by Curtis et al (5) in case of short fiber reinforced polyamide 6-6 matrix and a failure model has been elaborated. It was shown that strength enhancement

is limited by an embrittlement effect which reduces the strain to fracture as the stiffness of the composite is improved. The cause of this effect has been identified as matrix crack formation at the ends of the reinforcing fibers. Acoustic emission has shown that at low strains of between 0.5% and 1.0%, according to fiber type, length and V_f, cracks form at the tips of the longest fibres aligned in the straining direction. Subsequently, as the strain is increased, more cracks form progressively at the ends of shorter and/or more misaligned fibers. It has been shown that initially this cracking can be accommodated by load transfer to adjacent fibers which bridge the cracked region. Final failure occurs when the extent of cracking across the weakest section reaches a critical level, when the surrounding fibres and matrix can no longer support the increasing load.

Microscopic observation of the tensile fracture surfaces of the PBT and PP long fiber composites are shown in Figures 7 and 8, respectively. From these micrographs it can be observed that the mode of failure of these materials is complex and dependent of the fiber concentration. At low volume fraction of up to 11.1% for the PBT composites and 15.7% for the PP composites the failure mode is completely brittle. Brittle fracture was even observed for PP composite containing as low as 2.0% of long glass fiber (elongation at break of 2.45%) in spite of the fact that the pure PP matrix fractures in a purely ductile mode with an elongation at break of above 500%. The brittle behavior of PBT composites is nevertheless surprising since this matrix also fractures in a brittle mode

at strain of approximately 7%. As the fiber volume fraction increases, the fracture mode remains brittle but a complexe microscopic mode of fracture appears. On the fracture surface of the same sample, regions of ductile and brittle matrix fracture are observed. This observation can be easily made in sample of above 19% of glass fiber in case of PBT and above 15% in case of PP composite. Similar mode of fracture has also been reported by Bader _etal_ (4) in case of nylon 6 reinforced with E-glass fibers of number average fiber length of 370 μm. The ductile region was attributed to misaligned fibers and brittle region was found in case of well aligned fibers. However, the long fiber PBT composites exhibit a different fracture behavior. As opposed to nylon 6 or PP composite, ductility in the fracture surfaces was not observed in the misaligned fiber region but rather in the well aligned fiber region. Figure 9 shows micrographs of fracture surface of PBT and PP composites loaded in the transverse direction of the fiber axis. From this figure, it can be observed that misaligned fibers in PBT result in brittle fracture of the matrix. The difference in the mode of fracture between PBT and PP composites loaded in the transverse direction is most probably related to the difference in the fracture behaviors of these polymers. In fact, the stress in the composite loaded in the transverse direction is mainly supported by the matrix. Consequently, the mode of fracture will be the same as observed for the pure matrix: i.e. brittle fracture for PBT and ductile fracture for PP.

Furthermore, at high volume fraction of long fiber, the fracture surfaces show a higher microductility in both PP and PBT matrices, in spite of the fact that the macroscopic strain is reduced. This microductility is probably due to the increase in the number of fiber ends in the more concentrated samples.

Tensile Properties

Figure 10 shows the variation of the tensile modulus of the long fiber reinforced PP and PBT as a function of fiber volume fraction, V_f. The variation of the tensile modulus as a function of V_f was found to be linear up to approximately 36%. At higher volume fraction a negative deviation was observed. This deviation is most probably due to the decrease in fiber length and orientation in the highly filled materials as discussed above (see Figures 2,3, and 5). The variation of the tensile modulus as a function of V_f (the stiffness efficiency) was found to be more important in PBT than in PP composites, in spite of the fact that fiber lengths in PP are longer than those observed in PBT. Lower orientation and low level of adhesion in the PP composites are probably responsible for this phenomenon. It is well known that the tensile modulus of discontinuous fiber reinforced thermoplastic can be described by the modified law of mixtures:

$$E_c = K E_f V_f + E_m (1 - V_f) \qquad (1)$$

where K is a parameter depending on fiber alignment and fiber length in

the moulded samples. At low strain, it has been shown that the contribution of fiber length can be neglected (18). The behavior is essentially that of continuous fiber composite, but with misalignment accounted for. Consequently, the measurement of tensile modulus at very low strain could be used to evaluate the fiber orientation in the specimen. As discussed in (18), the orientation factor in case of uniaxial continuous composite is 1. For in-plane random fiber distribution it is decreased to a third and if the fibers are randomly disposed in three dimensions, this factor is 0.167. Figure 11 shows the values of the orientation factor determined for the PP and the PBT composites as a function of V_f. It can be observed that the fibers in the injection molded specimens are more aligned in the flow direction as expected. This factor also decreases as a function of fiber concentration as observed above (see Figure 5).

Figure 12 shows the variation of the ultimate tensile strengths as a function of fiber concentration. The ultimate strengths of both composites increase with increasing fiber concentration, attain a maximum and then decrease. At first sight, one could attribute the decrease observed in the case of the PP composite to the presence of holes in the moulded sample (see Figure 5). However, in the case of the PBT composites, voids are absent, even at very high fiber content in the samples. The drop in strengths of these composites should therefore be explained in terms of fiber length distribution, fiber orientation and interfacial bond strength. The composite strength could be expressed as (20):

$$\sigma_c^* = K\,\sigma_f^*\,V_f + \sigma_m'\,V_m \qquad (2)$$

where K is the parameter characterizing the fiber length and orientation, σ^*_c and σ^*_f are the failure strengths of the composite and the glass fiber, respectively, σ_m' is the stress in the matrix at composite failure strain. For discontinuous fiber composites, a critical fiber length, l_c, has been defined as the minimum length required for the stress in the fiber to be built up to its fracture strength:

$$l_c = r\,\sigma_f^*/\tau \qquad (3)$$

where r is the fiber radius and τ is the shear stress representing the fiber pull-out resistance. τ is related to either the shear strength of the matrix or the strength of the fiber/matrix interface.

From the definition of l_c all of those fibers with ends within a distance $l_c/2$ of the fracture surface will not break but will pull-out of the matrix. The strength at the interface can therefore be determined by the measurement of the maximum of fiber pull-out length as observed on the tensile fracture surface (19-25). To measure the pull-out length, samples of very low fiber content were used to insure that fibers are well oriented in the testing direction. In addition, fibers of length up to 10 mm are present in these samples. From the pull-out length measurement, the value of l_c obtained for the PP system is about ten times higher

than those which have been reported for glass/PP composites (3,19). The estimated interfacial shear strength obtained from equation (3) corresponding to the fiber pull-out measurement of the PBT (2.65 mm) and PP (4.6 mm) system are 7.12 MPa and 3.4 MPa, respectively.

The interfacial shear strength obtained from the fiber pull-out measurement of the diluted PP and PBT composites was used to predict the tensile strength of the highly filled composites. In the case of discontinuous fiber composites, the tensile strength is a function of fiber length. If the fiber length is shorter than l_c, the strength of the composite is given by (20):

$$\sigma_c^* = \eta_o (l/2r) V_f + \sigma_m' (1 - V_f) \quad (5)$$

where η_o is the orientation efficiency factor. If the fiber length is greater than l_c, the strength of the composite is given by the following equation (20):

$$\sigma_c^* = \eta_o (1 - l_c/2l) \sigma_f^* V_f + \sigma_m' (1 - V_f) \quad (6)$$

When fiber composites are processed by injection molding, the fiber alignment produced by resin flow leads to considerable fiber breakdown during the processing operations. Consequently, the fiber length in the moulded sample is not constant and shows very wide variations (see figures

2 and 3). In such cases some of the fibers are longer than l_c and some are shorter, combining equations (5) and (6) give (26):

$$\sigma_c^* = \eta_o \sum_{l_i < l_c} \frac{\tau\, l_i V_i}{2r} + \eta_o \sum_{l_j > l_c} \sigma_f^* V_j \left(1 - \frac{l_c}{2l_j}\right) + \sigma_m' (1 - V_f) \qquad (7)$$

where $$V_i + V_j = V_f$$

Following this development, the tensile strength of the long fiber reinforced PBT and PP can be predicted from the shear strength at the interface, τ, the fiber length distribution, and the critical fiber length and orientation.

The stress in the matrix, σ_m' at composite failure strain, ε_c was estimated using the assumption that in the composite, the strain of the matrix and the strain of the fiber are equal to the strain of the composite. σ_m' was then determined in the stress-strain curve of the pure polymer matrix at ε_c. The orientation factor, η_o was obtained from equation (1) as discussed above. Finally, σ_c^* was calculated using the fiber length distribution in the moulded sample by assuming that some fibers are shorter than l_c and some are longer than l_c which is evaluated from the fiber pull-out measurement. Results of these calculations are presented in Figure 12 for the PBT and PP long fiber composites tested in the direction parallel to the fiber axis. For a given glass fiber/polymer system, the prediction of σ_c^* is good except

for PP composites of composition of 36.4%. However, it is obvious that the presence of holes in this sample (Figure 5) results in a lower measured value of σ_c^*.

The calculated values of σ_c^* are near but systematically lower than the measured values of σ_c^* for the two systems. This result suggests that τ was underestimated. By measuring the pull-out length, the interfacial shear strength, τ, is evaluated for a system consisting of isolated fibers surrounded by matrix. Hence the corresponding τ represents the interfacial shear strength of one isolated fiber. However, in real samples the interface is not uniform for all fibers and, in addition, the shear resistance of the interface region between the fiber and the matrix may have different values at different points along the length of the fiber, due to imperfect adhesion. Consequently, fibers with poor bonding have lower interfacial strengths, higher l_c and consequently higher pull-out length. Hence, the use of the maximum length of fiber pull-out for the prediction of the tensile strength of the composites leads to a minimum value of σ_c^*. It should also be noted that the value of τ obtained for the PBT and PP long glass fiber composites is rather low and well below the maximum shear strength of the matrix suggesting imperfect bonding between fiber and matrix.

Long fiber reinforced PBT molded in form of a thick plates was used to investigate the effect of fiber orientation. In such thick injection molded samples, the long fibers are less aligned in the flow direction.

Figure 13 shows a schematic representation of the skin-core structure of the fiber orientation in the thick plate, as observed in scanning electron microscope. Two kinds of tensile specimen were cut from this thick plate. The first was obtained from the entire thickness and the second specimen was cut from the machined plate in which the skin layers have been removed. The latter contains therefore high degree of misalignment of fibers. Figure 14 to 16 show the tensile performances of the PBT composite versus fiber volume fraction at different levels of fiber alignment. As expected, an increase in fiber misalignment results in a reduction of the tensile properties. The results show that in 6 mm thick parts, no improvement of mechanical properties in the flow direction is observed over at least 3 mm in the core region. The decrease in tensile strength of the composite in this region (Figure 16) again confirms the poor fiber/matrix interfacial strength in the composite.

Calculated values of σ_c^* obtained from equation (1) and (7) are reported in Figure 16. Good agreement between measured and calculated values of σ_c^* for PBT composites over a wide range of compositions and orientation can be observed.

CONCLUSION

While injection moulding of long fiber pellets leads to composites in which the fiber length is much higher than that in conventional injection grades, significant fiber breakage occurs during injection moulding. Characterization of the fiber length distribution in the moulded samples

shows that the number average fiber length is reduced from about 12 mm to at least 2 mm. In addition, the fiber length decreases with increasing fiber content in the composites. High melt viscosity and high fiber contacts are probably responsible for the higher fiber breakage in the concentrated systems.

Critical fiber lengths, l_c, determined from the fiber pull-out measurements of PBT and PP composites are 5.28 mm and 9.2 mm, respectively. The value of l_c obtained for the long fiber reinforced PP system is almost ten times higher than those which have been reported to date (3,19) for glass/PP composites, either with good and poor bonding.

Using the measured l_c value and the modified rule of mixtures, the tensile strengths of the composites of various composition and fiber orientation can be accurately predicted. The l_c evaluation is supported by the good agreement observed between calculated and measured tensile strengths. Due to the high value of l_c, the weak performance of the PBT and PP composites is also attributed to the low interfacial strength in the composites. Optimum performance of these materials should be attained if significant amount of fibers longer than l_c are present in the composite. Consequently, greater attention should be made to optimize fiber/matrix adhesion and the injection moulding process of long fiber composites.

Table 1 - MATERIAL CHARACTERISTICS

PBT LONG FIBER COMPOSITES		PP LONG FIBER COMPOSITES	
V_f	l_{avg} [mm] (number)	V_f	l_{avg} [mm] (number)
4.9	1.77	2.0	--
11.1	--		
		7.9	2.18
19.0	1.18	15.7	1.68
33.9	1.00	36.4	0.88
45.0	--		
49.0	0.72		

REFERENCES

1) M.G. Bader and W.H. Bowyer, Composites, 4, 150 (1973).

2) J.M. Crosby and T.R. Drye, J. Reinf. Plast. Compos., 6, 162 (1987).

3) W.H. Bowyer and M.G. Bader, J. Mater. Sci., 7, 1315 (1972).

4) M.G. Bader and J.F. Collins, "Progress in Science and Engineering of Composites", T. Hayashi, K. Kawata & S. Umekawa, Ed., ICCM-IV, Tokyo, p. 1067 (1982).

5) P.T. Curtis, M.G. Bader and J.E. Bailey, J. Mater. Sci., 13, 377 (1978).

6) F. Ramsteiner and R. Theyson, Composites, - , 111 (1979).

7) M.W. Darlington, B.K. Gladwell and G.R. Smith, Polymers 18, 1269 (1977).

8) M.W. Darlington, P.L. McGinley, G.R. Smith, J. Mater. Sci., 11, 877 (1976).

9) J.C. Halpin, J. Compos. Mater., 3, 732 (1969).

10) L.E. Dingle, International Conference on Carbon Fibres, Their Place in Modern Technology, London, February 1974.

11) M.W. Darlington and G.R. Smith, Plast. Rubber, 3, 97 (1978).

12) M.J. Folkes, "Short Fibre Reinforced Thermoplastics", Research Studies Press, J. Wiley & Sons Ltd. (1982).

13) D. McNally, Polym. Plast. Technol. Eng., 8, 101 (1977).

14) S. Abrate, Rubber Chemistry and Technology, 59, 384 (1985).

15) B. Fisa, Polym. Compos., 6, 232 (1985).

16) B.D. Favis, J.P. Chalifoux and P. VanGheluwe, S.P.E. Techn. Papers, 33, 1326 (1987).

17) D.A. Cianelli, J.E. Travis and R.S. Bailey, Plastics Technology, April 1988, p.83.

18) H.L. Cox, Brit. J. Appl. Phys., 3, 72 (1952).

19) M.J. Folkes and W.K. Wong, Polymer, 28, 1309 (1987).

20) A. Kelly and W.R. Tyson, J. Mech. Phys. Solids, 13, 329 (1965).

21) A. Takaku and R.G.C. Arridge, J. Phys. D. Appl. Phys., 6, 2038 (1973).

22) L.J. Broutman and R.H. Krock (Eds). "Modern Composite Materials", Addison Wesley, New York, 1967.

23) J.D.H. Hughes, Applied Chem. Division, AERE, Harwell, 1977, Report No. R-8683.

24) L.T. Drzal, M.J. Rich, J.D. Camping and W.J. Park, "35th Annu. Tech. Conf. Reinforced Plastics/Composites Institute, The Society of the Plastics Industry, Inc., 1980.

25) P.S. Chua and M.R. Piggott, Compos. Sci. Tech., 22, 33 (1985).

26) A. Kelly and N.H. MacMillan, "Strong Solids", Clarendon Press (1986).

FIGURE CAPTIONS

Figure 1 - Fiber dispersion and impregnation in long fiber pellets a) PBT long fiber pellets, b) PP long fiber pellets.

Figure 2 - Fiber length distribution in long fiber reinforced PBT of various compositions.

Figure 3 - Fiber length distribution in long fiber reinforced PP of various compositions.

Figure 4 - Micrographs of fractured surfaces of long fiber reinforced PBT of composition of (a) 4.9% and (b) 11.1% obtained by dilution of pellets of 54%.

Figure 5 - Micrographs of polished surfaces of tensile specimens (ASTM D638 Type 1) of PBT and PP long fiber composites of various compositions.

Figure 6 - Percentage of elongation at break of long fiber reinforced PP and PBT as a function of fiber volume fraction.

Figure 7 - Micrographs of tensile fractured surfaces of long fiber reinforced PBT of composition of a) 4.9% and b) 49%.

Figure 8 - Micrographs of tensile fractured surfaces of long fiber reinforced PP of composition of a) 7.9%, b) 15.7% and c) 36.4%.

Figure 9 - Micrographs of fractured surfaces of a) PBT and (b) PP composites loaded in the transverse direction of the fiber axis.

Figure 10 - Young's modulus of long fiber reinforced PP and PBT as a function of fiber volume fraction.

Figure 11 - Orientation factor of injection molded samples of long fiber reinforced PP and PBT calculated from the modified rule of mixtures, as a function of fiber volume fraction.

Figure 12 - Ultimate tensile strength of long fiber reinforced PP (o, •) and PBT (Δ, ▲) as a function of fiber volume fraction.

Figure 13 - Schematic representation of fiber orientation in injection thick plate.

Figure 14 - Percentage of elongation at break of long fiber reinforced PBT of different levels of fibers alignment. (o); injected tensile specimen ASTM-D638 Type 1, (□); entire thick plate, (▽); core section of the thick plate.

Figure 15 - Young's modulus of long fiber reinforced PBT of different levels of fiber alignment. (o); injected tensile specimen ASTM D-638 Type 1, (□); entire thick plate, (Δ); core section of the thick plate.

Figure 16 - Ultimate tensile strength of long fiber reinforced PBT of different levels of fiber alignment. (o); injected tensile specimen ASTM D-638 Type 1, (□); entire thick plate, (Δ); core section of the thick plate.

(b)

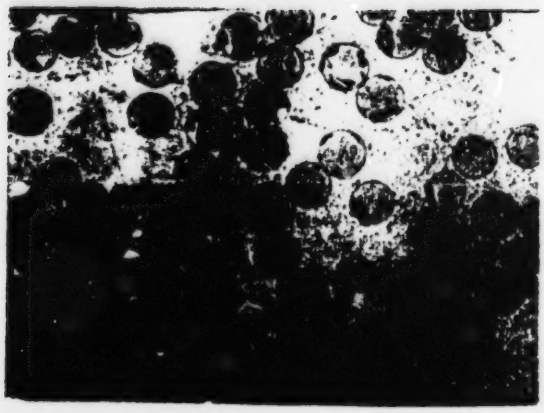

(a)

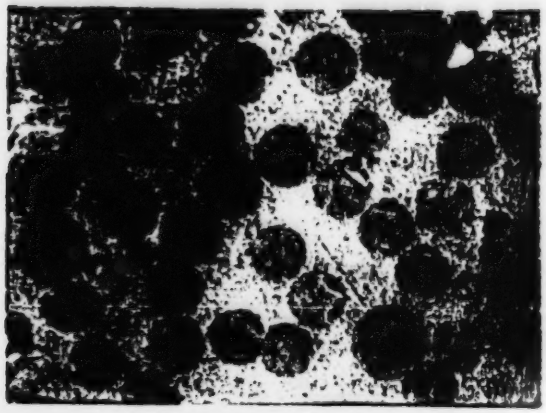

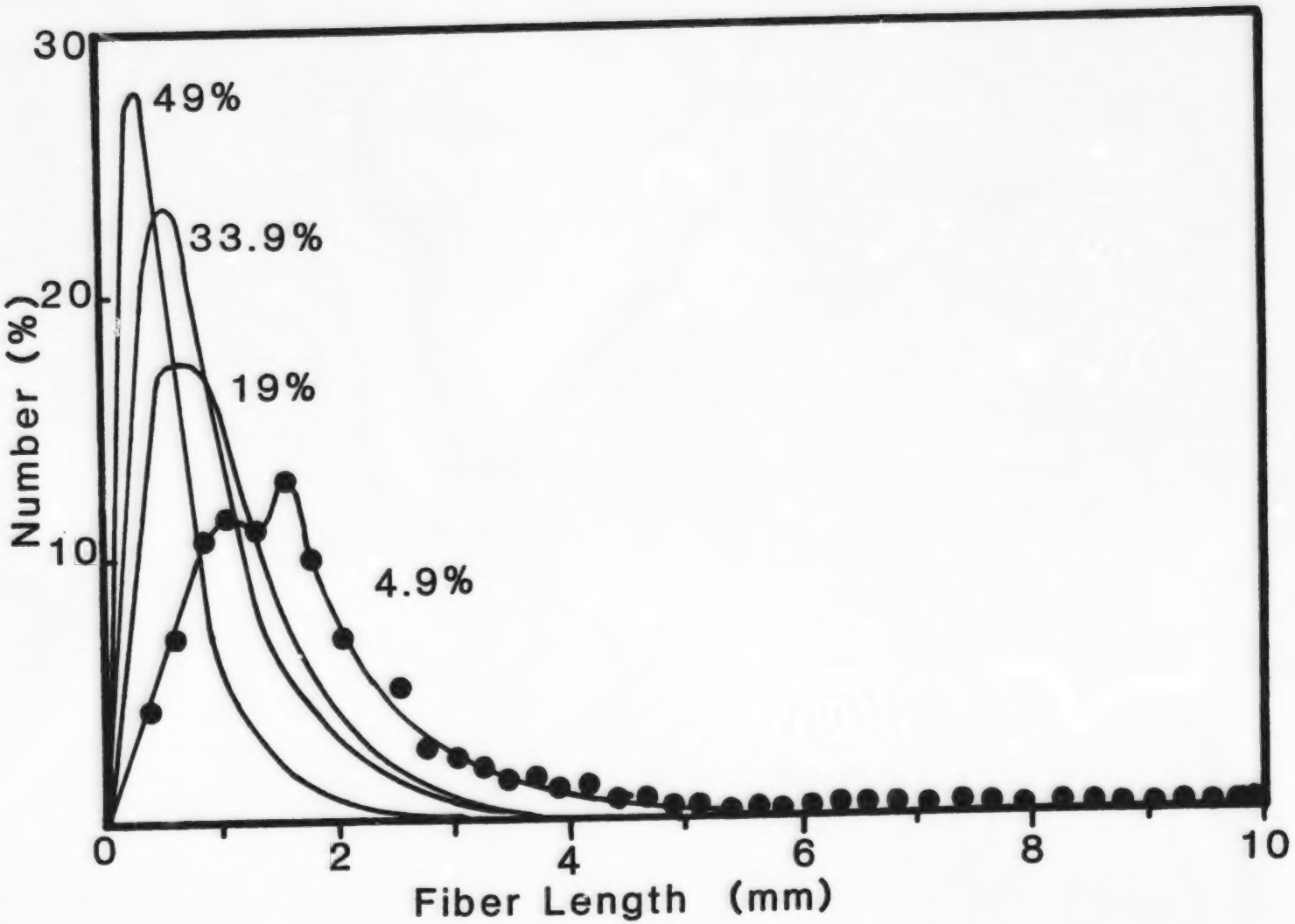
30
20
10
Number (%)
49%
33.9%
19%
4.9%
0
2
4
6
8
10
Fiber Length (mm)

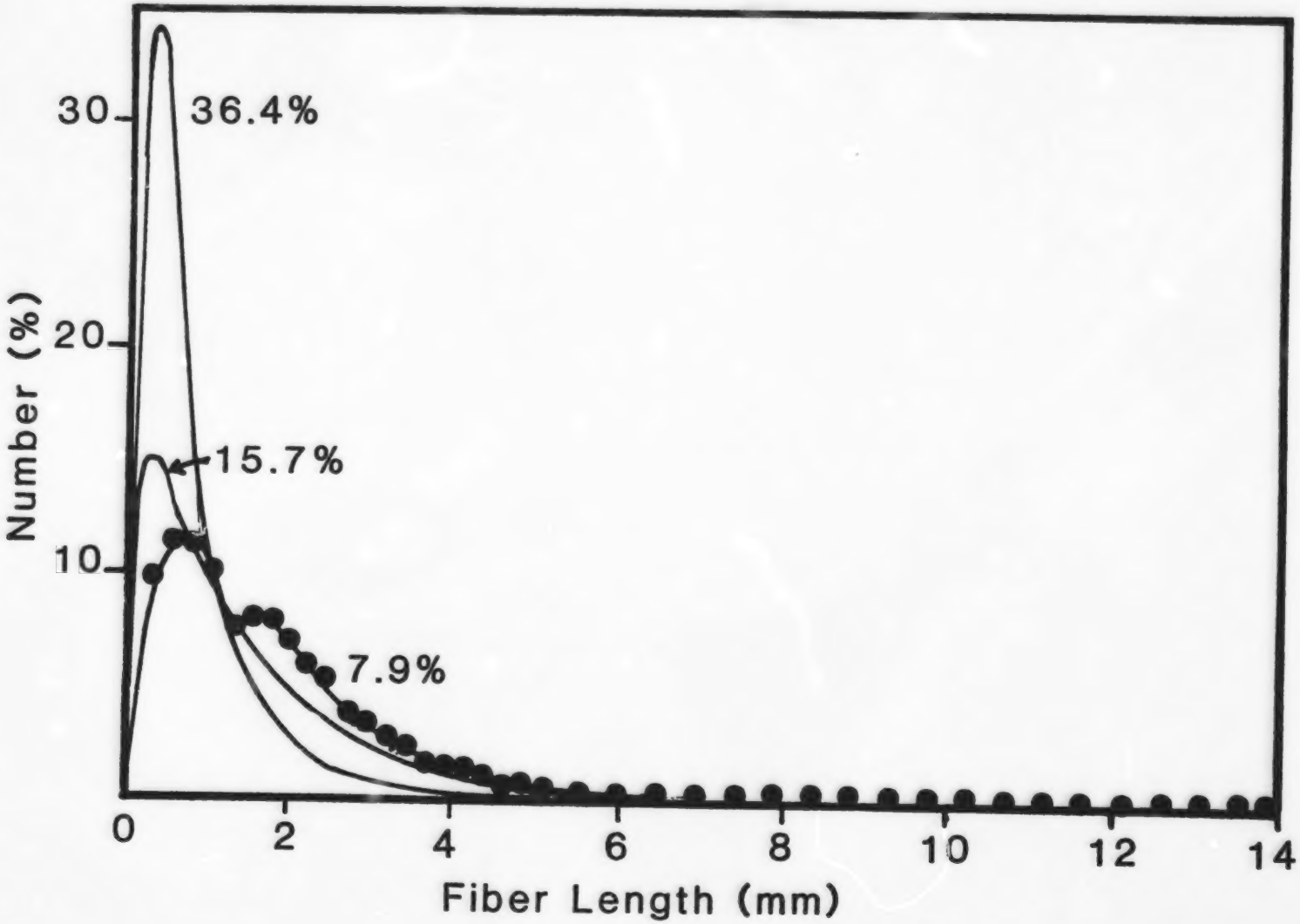
30
20
10
Number (%)
36.4%
15.7%
7.9%
0
2
4
6
8
10
12
14
Fiber Length (mm)

(b)

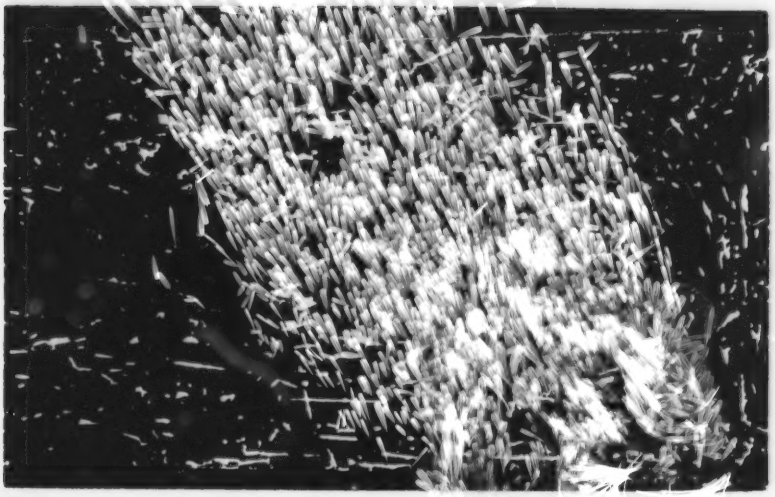

(a)

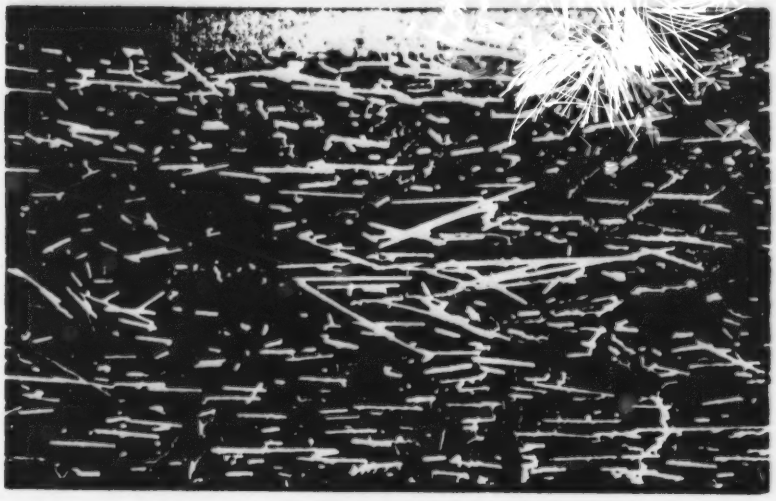

49%

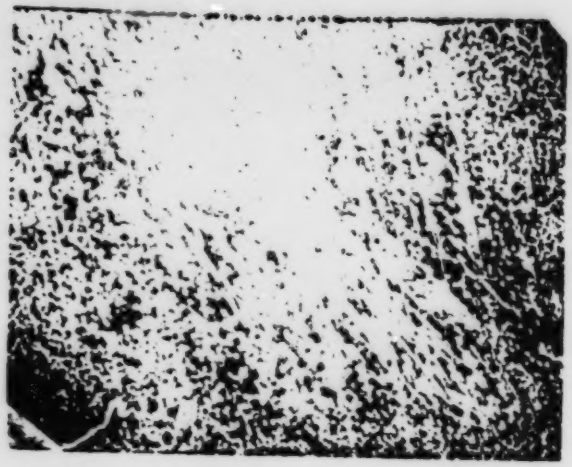

36.4%

11.1%

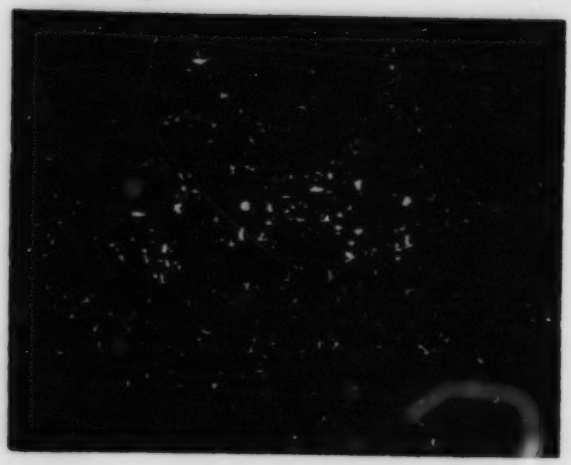

15.7%

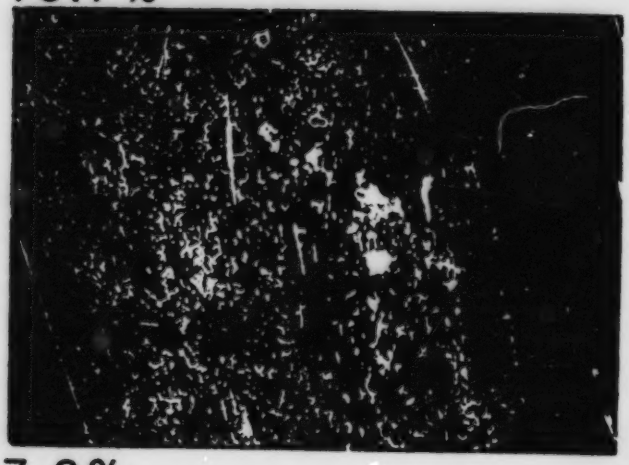

4.9%

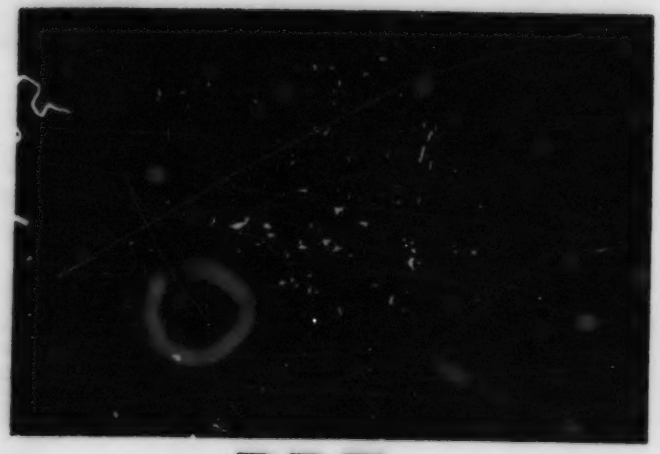

PBT

7.9%

PP

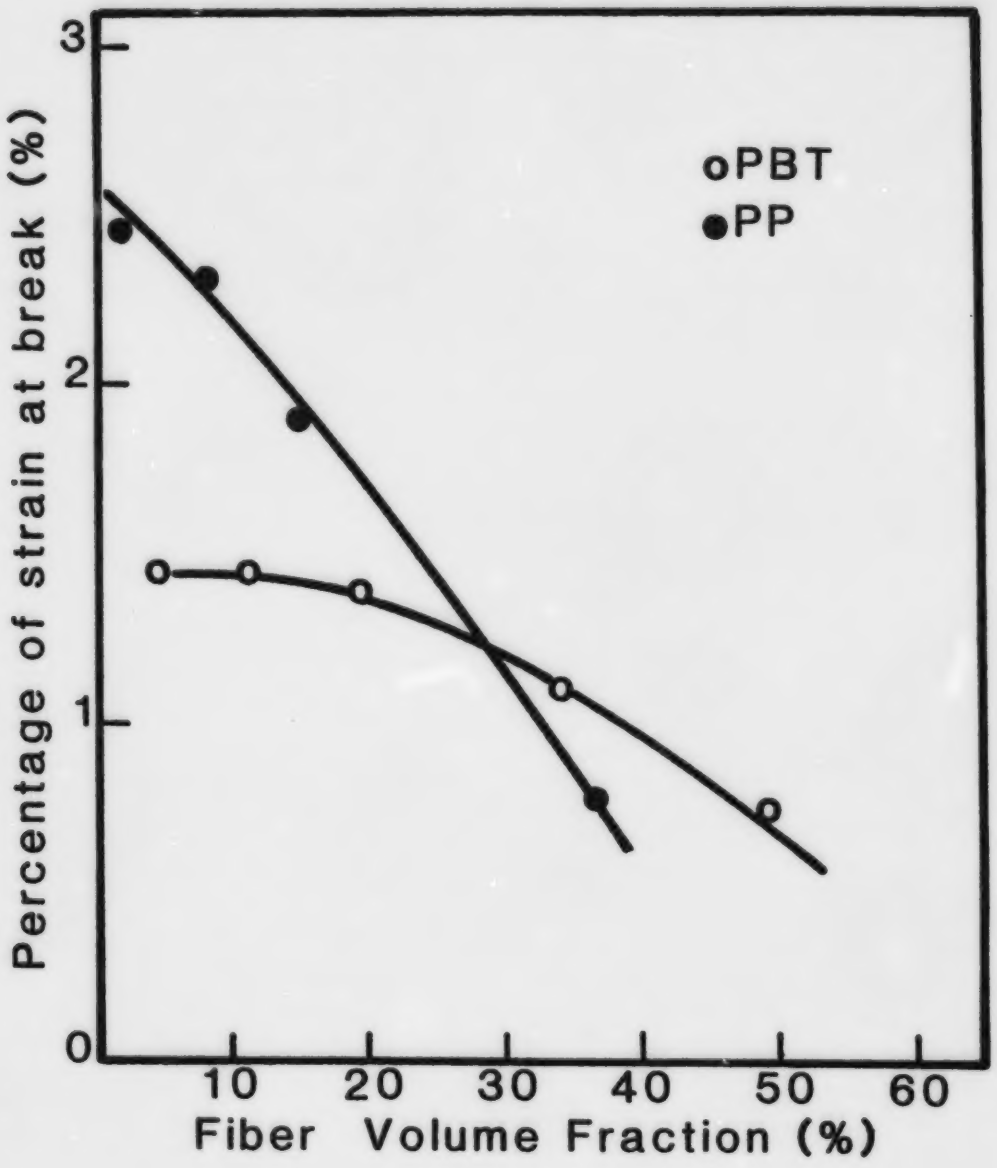
Percentage of strain at break (%)
3
2
1
0
oPBT
●PP
10
20
30
40
50
60
Fiber Volume Fraction (%)

(a)

(b)

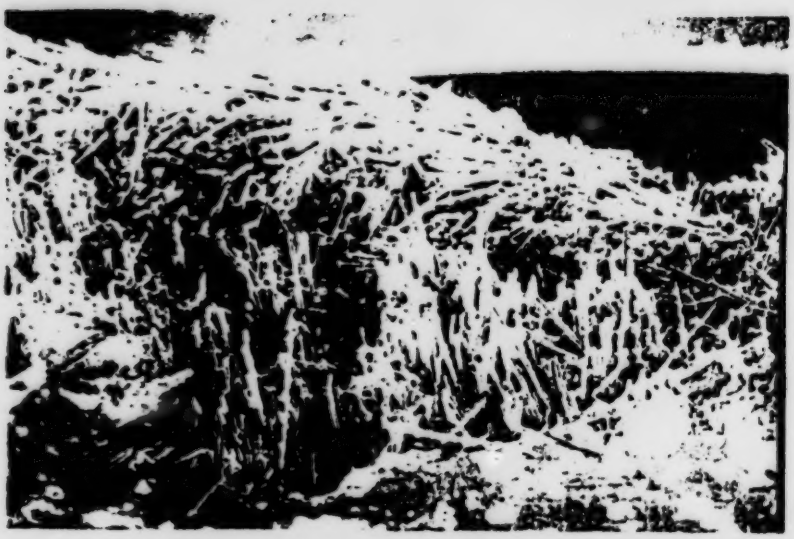

(a)

(b)

(c)

(a)

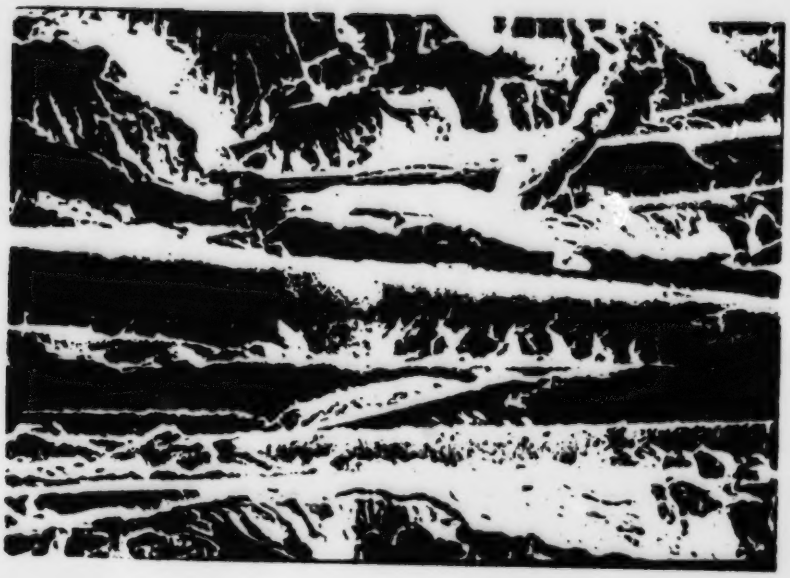

(b)

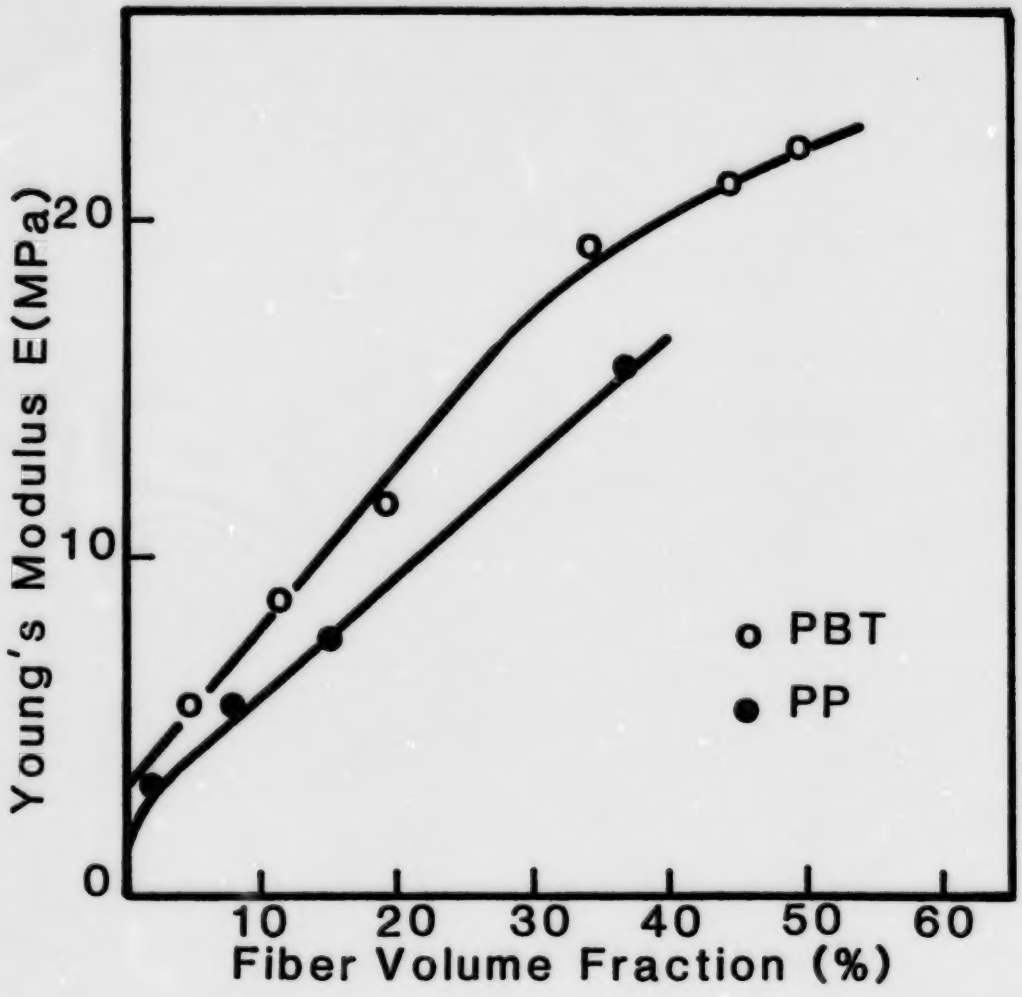
Young's Modulus E(MPa)
20
10
0
10
20
30
40
50
60
Fiber Volume Fraction (%)
o PBT
● PP

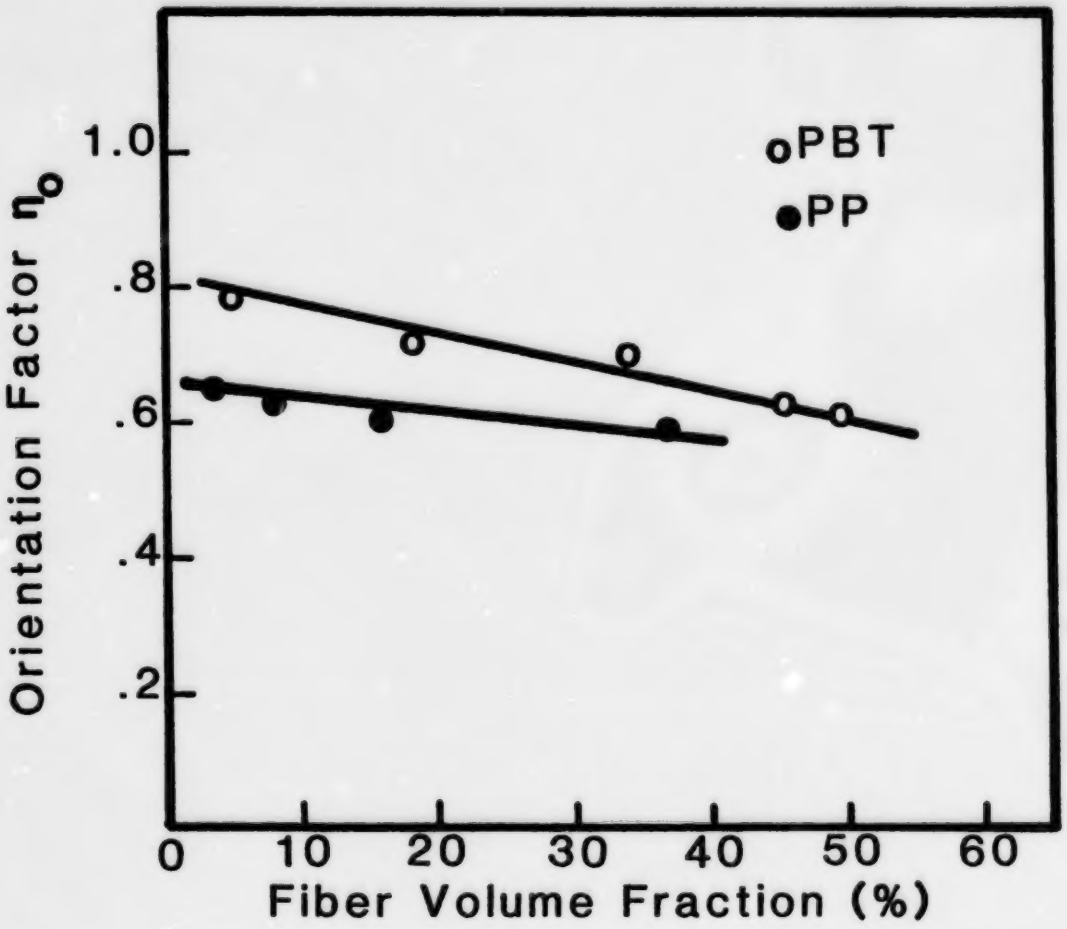
Orientation Factor η_o
1.0
.8
.6
.4
.2
0
10
20
30
40
50
60
Fiber Volume Fraction (%)
oPBT
●PP

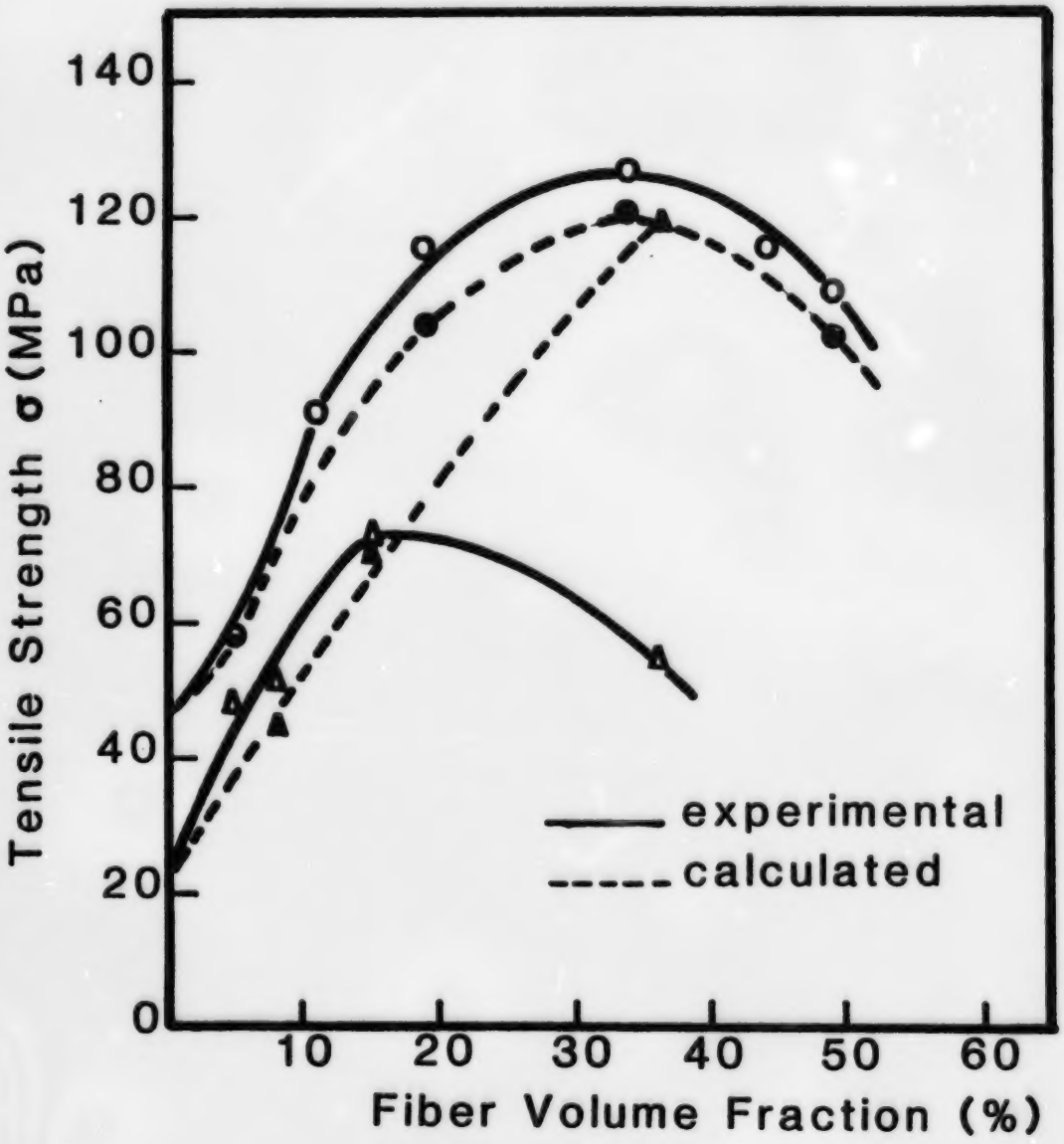
Tensile Strength σ (MPa)
140
120
100
80
60
40
20
0
10
20
30
40
50
60
Fiber Volume Fraction (%)
experimental
calculated

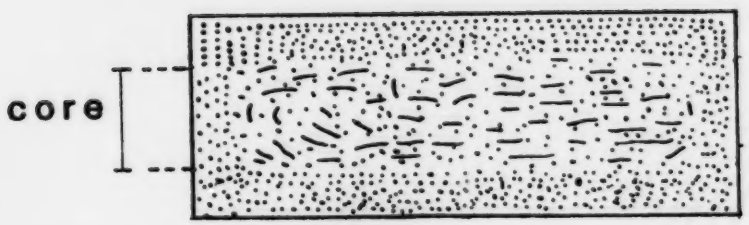
core

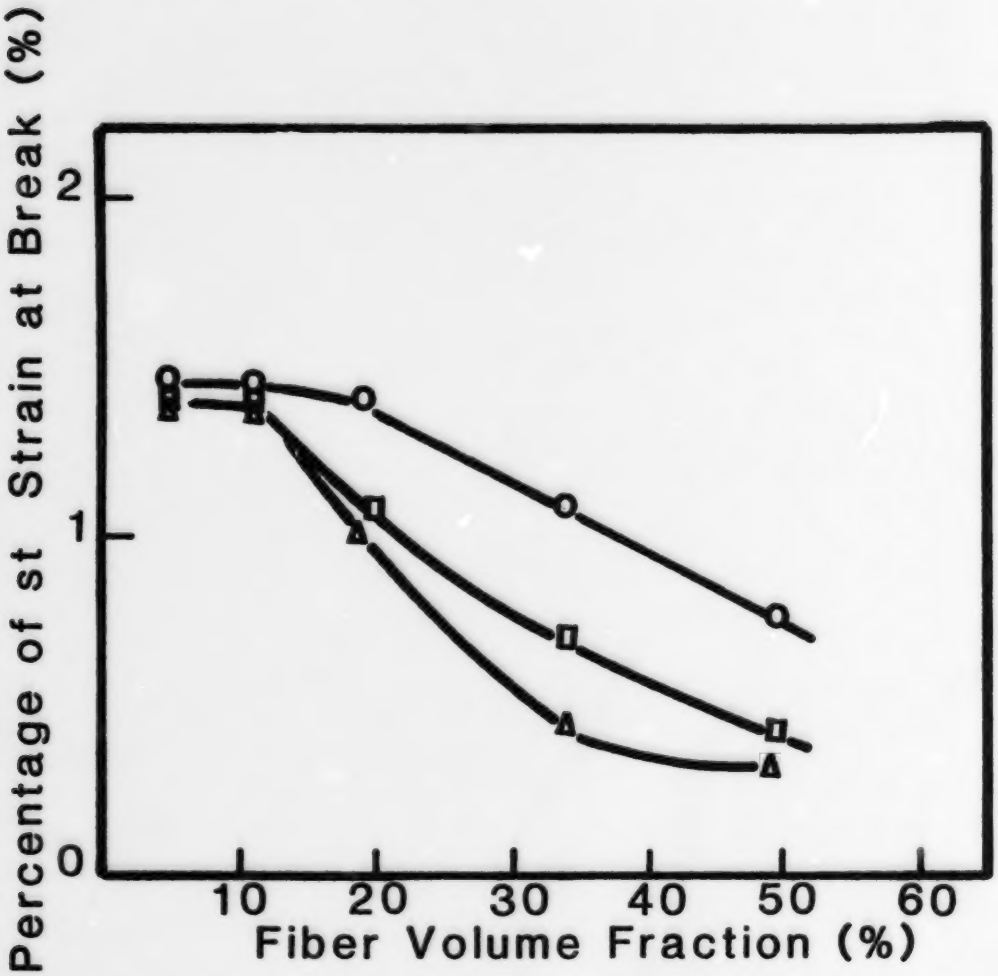
Percentage of st Strain at Break (%)
2
1
0
10
20
30
40
50
60
Fiber Volume Fraction (%)

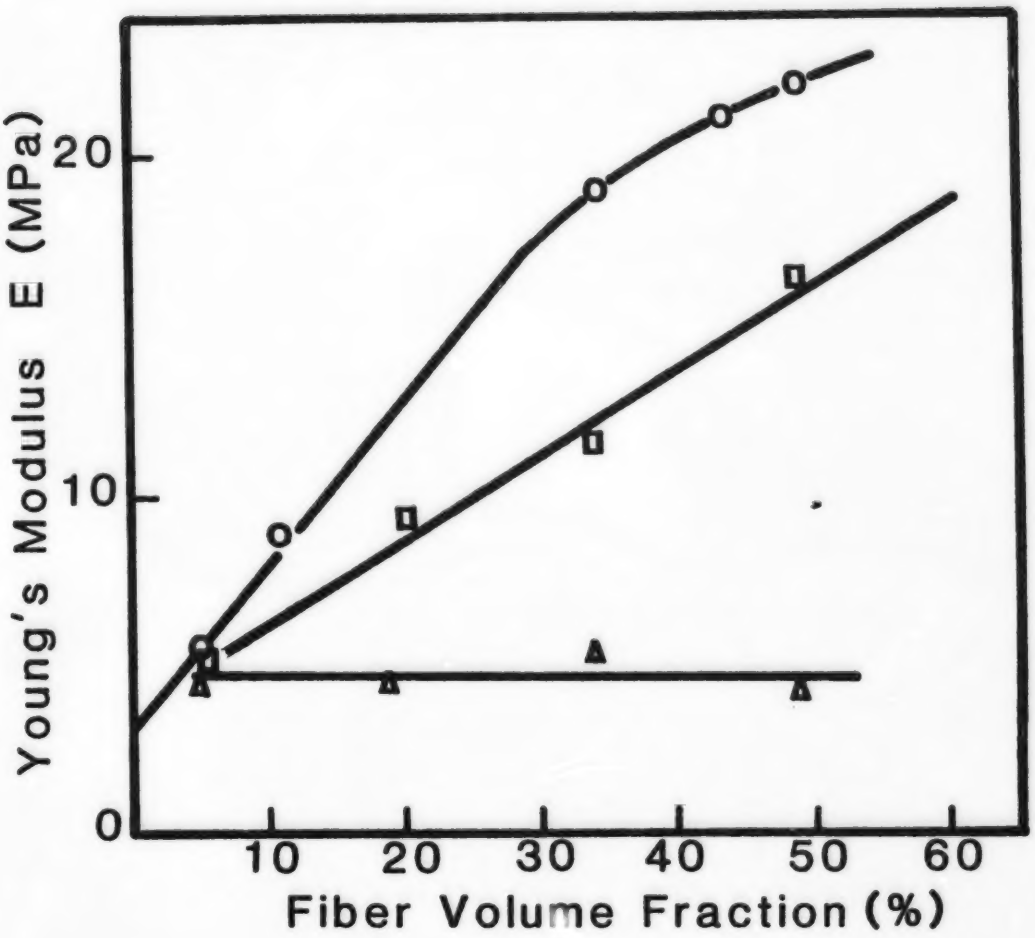
Young's Modulus E (MPa)
20
10
0
10
20
30
40
50
60
Fiber Volume Fraction (%)

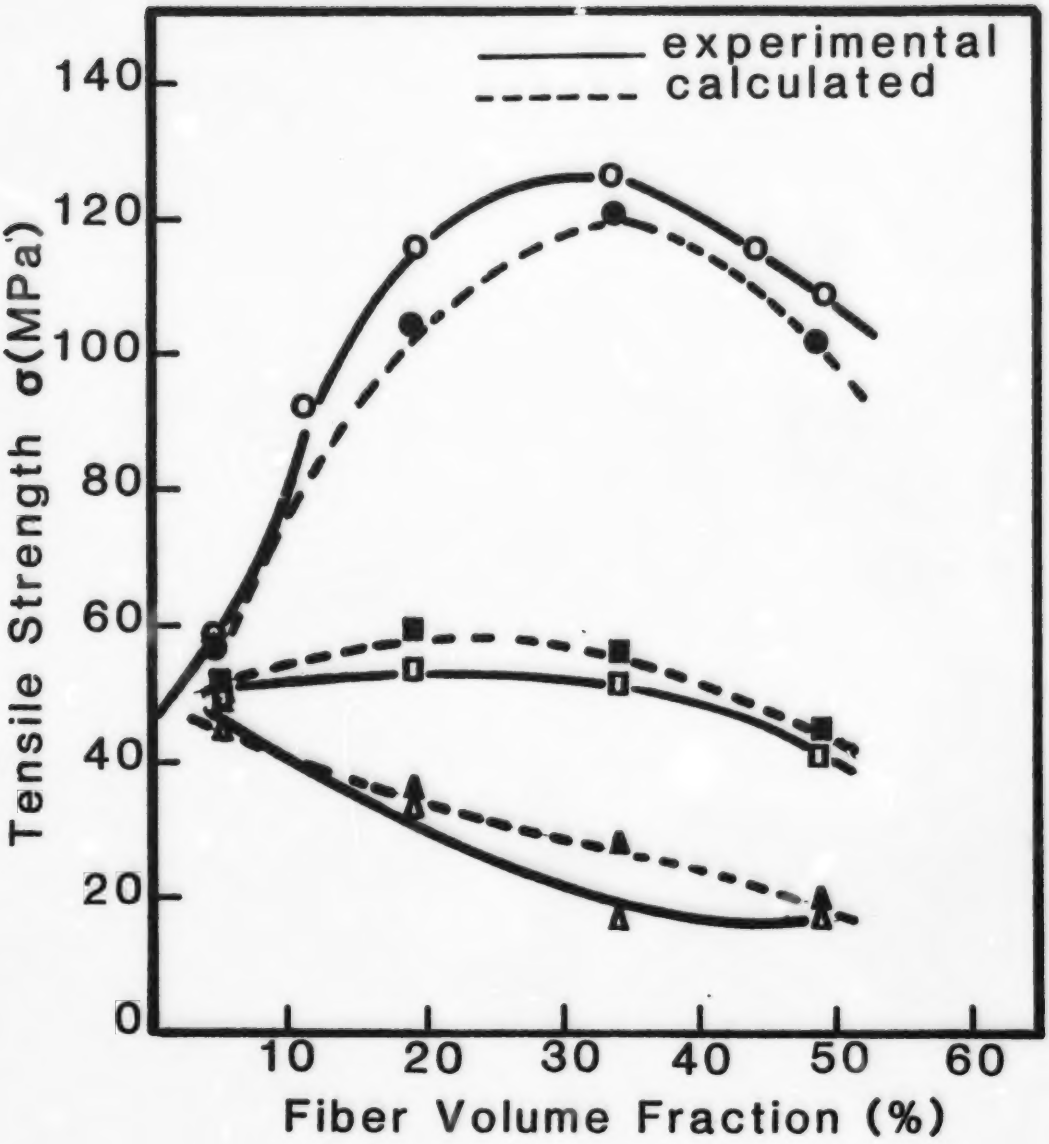
experimental
calculated
Tensile Strength σ(MPa)
140
120
100
80
60
40
20
0
10
20
30
40
50
60
Fiber Volume Fraction (%)